LA-UR-14-21466
Approved for public release; distribution is unlimited.

Title: Total Cross Sections as a Surrogate for Neutron Capture: An Opportunity to Accurately Constrain (n,) Cross Sections for Nuclides Beyond the Reach of Direct Measurements

Author(s): Koehler, Paul E.

Intended for: Description of potential new capability at LANSCE
Report

Issued: 2014-03-05

Total Cross Sections as a Surrogate for Neutron Capture: An Opportunity to Accurately Constrain (n,γ) Cross Sections for Nuclides Beyond the Reach of Direct Measurements

P. E. Koehler*
LANSCE-NS
(Dated: September 12, 2013)

There are many (n,γ) cross sections of great interest to radiochemical diagnostics and to nuclear astrophysics which are beyond the reach of current measurement techniques, and likely to remain so for the foreseeable future. In contrast, total neutron cross sections currently are feasible for many of these nuclides and provide almost all the information needed to accurately calculate the (n,γ) cross sections via the nuclear statistical model (NSM). I demonstrate this for the case of ^{151}Sm; NSM calculations constrained using average resonance parameters obtained from total cross section measurements made in 1975, are in excellent agreement with recent ^{151}Sm(n,γ) measurements across a wide range of energy. Furthermore, I demonstrate through simulations that total cross section measurements can be made at the Manuel Lujan Jr. Neutron Scattering Center at the Los Alamos Neutron Science Center for samples as small as 10 μg. Samples of this size should be attainable for many nuclides of interest. Finally, I estimate that over half of the radionuclides identified ~ 20 years ago as having (n,γ) cross sections of importance to s-process nucleosynthesis studies (24/43) and radiochemical diagnostics (11/19), almost none of which have been measured, can be constrained using this technique.

I. INTRODUCTION

There are many radionuclides for which (n,γ) cross sections are of great interest to radiochemical diagnostics and to nuclear astrophysics, but which are beyond the reach of current, or foreseeable future, direct measurement techniques. The main problem with direct measurements is that background from decay of the radioactive sample overwhelms the signal from (n,γ) events. In contrast, total neutron cross sections currently are feasible for many of these nuclides and provide almost all the information needed to accurately calculate the (n,γ) cross sections via the nuclear statistical model (NSM). I demonstrate this for the case of ^{151}Sm; NSM calculations constrained using average resonance parameters obtained from total cross section measurements made in 1975, are in excellent agreement with recent ^{151}Sm(n,γ) measurements across a wide range of energy. Furthermore, I demonstrate through simulations that total cross section measurements can be made at the Manuel Lujan Jr. Neutron Scattering Center (MLNSC) at the Los Alamos Neutron Science Center (LANSCE) for samples as small as 10 μg. Samples of this size should be attainable for many nuclides of interest.

II. CONSTRAINING CAPTURE WITH TRANSMISSION (TOTAL CROSS SECTION) MEASUREMENTS

In this section, I demonstrate for the test nuclide ^{151}Sm, that resonance parameters obtained from analysis of a total neutron cross section measurement made in 1975 can be used to obtain the capture cross section to an accuracy on par with direct measurements made 30 years later.

According to the NSM, the average neutron capture cross section due to s waves can be written as,

$$\langle\sigma\rangle = \frac{2\pi^2}{k^2}\frac{S_0\langle\Gamma_\gamma\rangle/D_0}{S_0+\langle\Gamma_\gamma\rangle/D_0}W, \tag{1}$$

where the wave number is $k(\mathrm{cm}^{-1}) = 2.1968\times 10^9(\frac{A}{A+1})\sqrt{E(\mathrm{eV})}$, and W is the width-fluctuation correction factor. All three of the parameters needed for Eq. 1 can be determined from $\mathcal{R}$-matrix analysis of the total neutron cross section, from which resonance energies E_0, reduced neutron widths $g\Gamma_n^0$ (where $g = (2J+1)/((2I+1)(2j+1))$, where J, I, and j are the spins of the resonance, target, and neutron, respectively, is the statistical spin factor), and radiation widths $\Gamma_\gamma$are extracted by fitting the observed resonances. For example, the s-wave neutron strength function S_0 is defined as,

$$S_0 = \frac{\langle g\Gamma_n^0\rangle}{D_0} = \frac{\sum g\Gamma_n^0}{\Delta E}, \tag{2}$$

and usually is determined from the slope of a plot of the cumulative reduced neutron width $\sum g\Gamma_n^0$ versus E_0. Similarly, the average s-wave resonance spacing D_0 typically is determined from the inverse of the slope of a plot of the cumulative number of resonances versus E_0. Lastly, a weighted (by inverse variance) average of the observed total radiation widths Γ_γ yields the average radiation width $\langle\Gamma_\gamma\rangle$. W corrects for the large variations in the $g\Gamma_n^0$ values due to the inherent Porter-Thomas fluctuations [1], and several methods (e.g., see [2]) have been devised for its calculation.

*Electronic address: koehler@lanl.gov

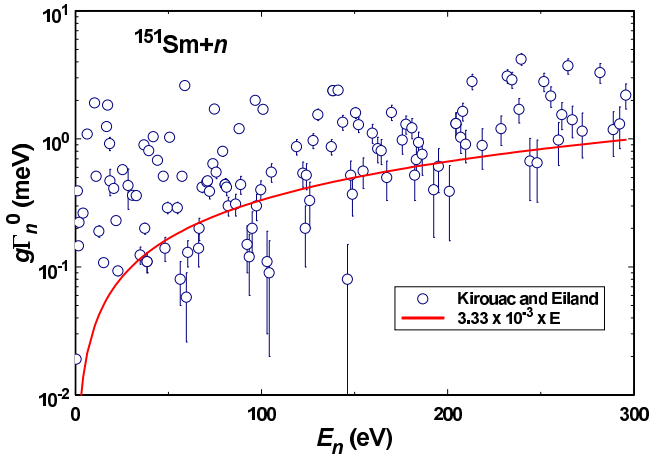

FIG. 1: Energy-reduced widths for ^{151}Sm neutron resonances from Ref. [3] (open blue circles). The red curve depicts the threshold used for obtaining corrected average resonance spacing (D_0) and neutron strength function (S_0) values. See text for details.

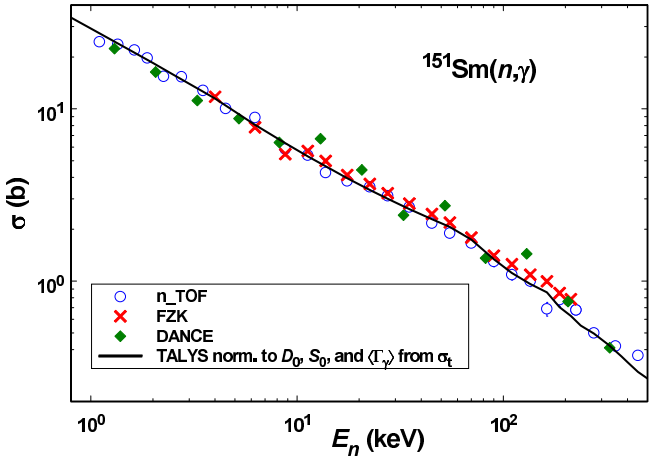

FIG. 2: ^{151}Sm(n,γ) cross section in the unresolved-resonance range. Symbols depict results from three different measurements [7–9], and the solid black curve is the cross section predicted by TALYS after adjustment to the average resonance parameters determined from the earlier ^{151}Sm+n total cross section measurement [3].

Transmission measurements on a 204.1-mg sample of ^{151}Sm, made at the Rensselaer Polytechnic Institute (RPI) electron linear accelerator facility, were reported in 1975 [3]. Data were obtain for $E_n = 0.01$ eV to 2.5 keV using a flight path length of 31.6 m, an electron burst width of 60 ns, and an accelerator repetition rate of 550 Hz.

By fitting the data, parameters E_0 and $g\Gamma_n^0$ were obtained for 120 resonances below 300 eV. In addition, Γ_γ values were obtained for 13 of the 14 lowest-energy resonances. The reduced neutron widths as a function of resonance energy are shown in Fig. 1. Apart from the inherent Porter-Thomas fluctuations [1], the $g\Gamma_n^0$ values should be, on average, independent of energy.

However, as can be seen in Fig. 1, fewer small resonances are observed as the energy increases. This well-known inherent experiment effect must be taken into account in order to obtain the correct D_0 and S_0 values from the data. I applied the technique of Ref. [4], using the threshold shown in Fig. 1, to obtain $D_0 = 1.1 \pm 0.07$ eV and $S_0 = 3.58 \pm 0.59$. Uncertainties for D_0 and S_0 were calculated according to Ref. [5]. An "error weighted" value of $\langle\Gamma_\gamma\rangle = 96$ meV is given in Ref. [3]. From the 13 Γ_γ values in this reference, I calculated a (inverse-variance) weighted average of $\langle\Gamma_\gamma\rangle = 96.5 \pm 1.4$ meV.

I used the NSM code TALYS (version 1.4) [6] to calculate the ^{151}Sm(n,γ) cross section. Using the default level-density model (constant temperature plus Fermi gas), I adjusted the $a(S_n)$ parameter from a default value of 23.20594 to 23.1 to obtain $D_0 = 1.1$ eV. Next, I adjusted the neutron optical model potential (NOMP) parameters to obtain $S_0 = 3.50$ (and $S_1 = 1.50$). To obtain these values, I had to adjust the depth and diffuseness parameters of the real part of the NOMP by factors of 0.9 and 1.336, respectively. Finally, I used the "gamgam 62 152 0.096" option in TALYS to normalize the photon strength function for ^{152}Sm to the measured $\langle\Gamma_\gamma\rangle$. As can be seen in Fig. 2, the resultant TALYS prediction is in excellent agreement with the available ^{151}Sm(n,γ) cross-section data [7–9].

III. FUTURE TOTAL-CROSS-SECTION MEASUREMENTS AT THE MLNSC

A schematic diagram of the transmission apparatus at the Oak Ridge Electron Linear Accelerator (ORELA) is shown in Fig. 3. In principle, a transmission experiment is among the simplest and least prone to systematic errors possible; there is no need to measure the absolute flux, detector efficiency, etc., and the only significant systematic uncertainty is related to the sample thickness. The flux transmitted through the sample T is related to the total cross section for the sample σ by the equation $T = e^{-n\sigma}$, where n is the sample thickness. Because there are other materials in addition to the sample between the neutron source and detector, the transmitted fluxes for both the sample and a empty sample holder are measured. Then, the (flux normalized) ratio of the transmitted flux with the sample in the beam to the transmitted flux through the empty holder is equal to the transmission through the sample alone. In practice, the sample and its holder are cycled in and out of the beam on a time scale on the order of 10 minutes to eliminate systematic errors due to detector and flux-monitor gain shifts, changes in background conditions, etc.

The measurements on which the above calculation was based were made at a facility whose flux was orders of magnitude smaller than that available at the MLNSC. Scaling from the measured flux [10] on flight path 4 and

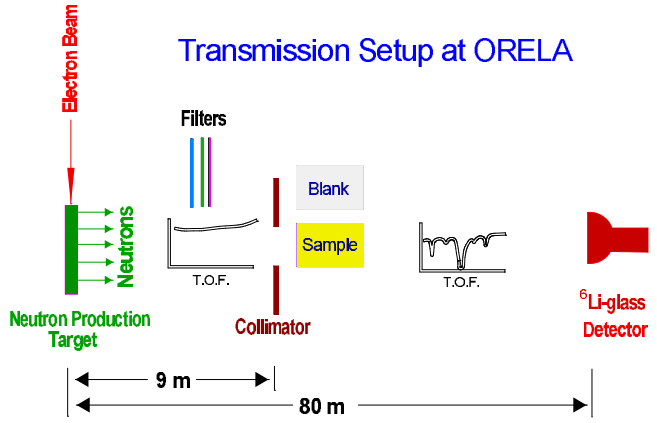

FIG. 3: Schematic (not to scale) diagram of the transmission apparatus at the ORELA. A 150-MeV pulsed electron beam from the accelerator impinged on a water-cooled tantalum neutron-production target. The flux coming off the target is realtively smooth as a function of time of flight, but after it passes through the sample, there are a number of dips due to resonances. A ^{6}Li-glass scintillator coupled to a photomultiplier tube was used to detect neutrons transmitted through the sample. The sample is periodically exchanged with a blank, and black-resonance filters to determine backgrounds. Typically, lead and boron filters were permenantly in the beam to reduce γ-flash effects and wrap-around neutrons, respectively.

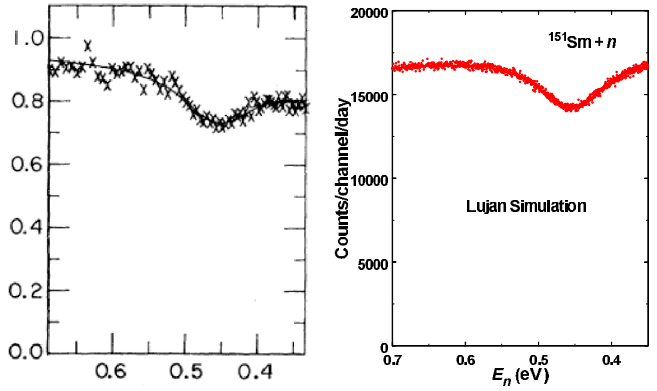

FIG. 4: Comparison of measured (X's) and fitted (solid curve) transmissions from Ref. [3] (left) to simulated sample-in counting rate (right) for a transmission experiment at the MLNSC using a 100-μg sample of ^{151}Sm. See text for details.

the estimated flux used in Ref. [3], I calculated that measurements of similar quality on the same nuclide could be made at the MLNSC with a sample as small as 7 μg.

To verify this estimate, I wrote a code to calculate the counting rate expected based on the measured flux [10] and measured efficiency for a neutron detector which is assumed to be a 1.27-cm thick GS20 ^{6}Li-glass scintillator [11]. The flux was scaled by $(d_0/d)^2$, where d_0 is the flight path length used in the actual flux measurements and d is the flight path length for the simulated experiment. The counting rate was obtained from the flux according to the sample diameter, assuming the sample is halfway between the source and the detector and that all neutrons transmitted through the sample hit the detector.

Simulation results for a 100-μg ^{151}Sm sample are shown in Figs. 4–7. Transmission versus neutron energy from the measurements of Ref. [3] are shown on the left or top panels of each of these figures. The right or bottom panels of Figs. 4–7 depict simulated counts/channel/day. Channel widths were calculated to be equal to one resolution width assuming a pulse width from the proton storage ring of 125 ns and a moderation time spread in μs equal to $\Delta t_m = 1.5/\sqrt{E}$, for neutron energy E in eV. The simulations assumed a flight path length of $d = 60$ m and the same sample thickness (2.858×10^{-4} at/b) used in Ref. [3]. Assuming negligible background, perfect alignment, etc., the same rates would be expected for a 10-μg sample in 10 days time. Statistical fluctuations in the counting rates were calculated by sampling from normal distributions with standard deviations equal to the square root of the average counting rate for each channel.

For the simulations, the $\mathcal{R}$-matrix code SAMMY [12] was used to calculate the total ^{151}Sm+n cross section from the resonance parameters of Ref. [3], using the MLNSC resolution function determined with the Detector for Advanced Neutron Capture Experiments (DANCE). As can be seen from Figs. 4–7, the statistical precision predicted by the simulations often is much better than in the measurements of Ref. [3], especially considering that there often are fewer channels in the measured spectra.

There were approximately 10^8 counts/day, or 58 counts/pulse for E_n = 0.3–300 eV for this simulation, corresponding to an average of 130 μs between events.

IV. CHALLENGES

The simulations indicate that experiments are feasible with samples as small as 10 μg. Nevertheless, there are several challenging aspects to an actual experiment, 3 of which are discussed in the following subsections. Most of these challenges could be addressed by test measurements with inexpensive, stable samples.

A. The sample

The sample likely represents the most challenging aspect of the experiment. On the other hand, sample requirements for a transmission experiment are considerably more relaxed than those for capture or fission. For example, because the detector is tens of meters away from the sample and can be made inherently insensitive to γ rays, the sample for transmission measurements can be much more radioactive than that for capture. In addition the sample container for transmission can be more

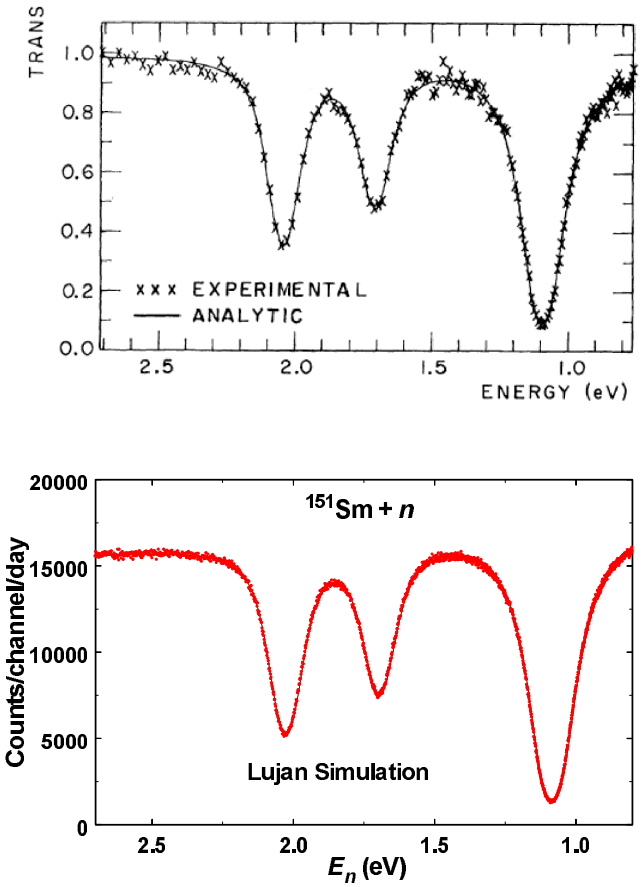

FIG. 5: Comparison of measured [3] transmission (top) to simulated sample-in counting rate (bottom) for a transmission experiment at the MLNSC using a 100-μg sample of ^{151}Sm. See text and caption of Fig. 4 for details.

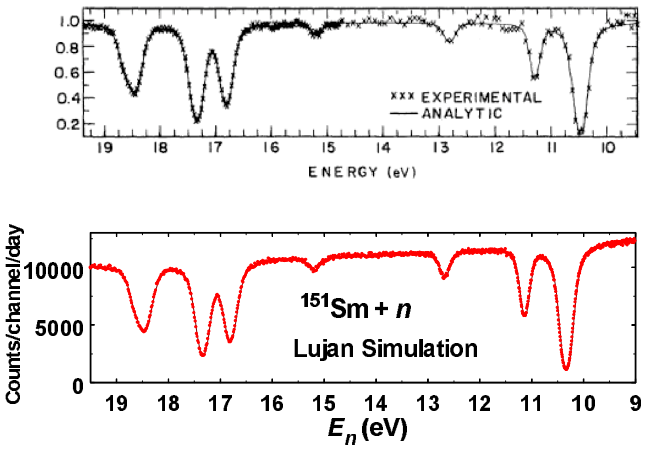

FIG. 6: Comparison of measured [3] transmission (top) to simulated sample-in counting rate (bottom) for a transmission experiment at the MLNSC using a 100-μg sample of ^{151}Sm. See text and caption of Fig. 4 for details.

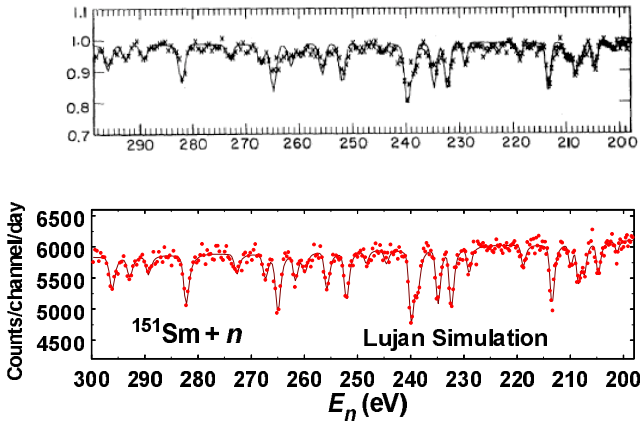

FIG. 7: Comparison of measured [3] transmission (top) to simulated sample-in counting rate (bottom) for a transmission experiment at the MLNSC using a 100-μg sample of ^{151}Sm. The solid red curve in the bottom panel represents the simulated average counting rate. See text and caption of Fig. 4 for details.

massive and robust, and even liquid samples are possible (and sometimes may be preferred).

Because the main goal of the experiment is to measure parameters for as many resonances of the isotope of interest as possible, the sample should be as highly enriched as possible. This requirement can be circumvented to some extent by extra measurements for the contamination isotopes and/or measurements on the same sample at times spaced far enough apart that the isotopic composition of the sample has changed substantially due to radioactive decay.

The sample should be uniform. This may be challenging for such small samples. In the past, using a liquid "carrier" in which the isotope of interest (or a chemical compound containing the isotope) will dissolve has been used to circumvent this problem. The carrier should have no or very few resonances in the region of interest. Water may be a good choice.

The thickness (number of atoms/barn) of the sample needs to be known with good accuracy as this parameter directly affects all of the resonance parameters determined in the resonance analysis. This requirement may be circumvented if the sample isotopics are well known and at least one of the contamination isotopes has one or more resonances which can be used to calibrate the sample thickness.

B. Positioning and alignment errors

In a typical transmission experiment, the sample and an empty sample holder are cycled in and out of the beam on a time scale on the order of 10 minutes. This is done to reduce possible systematic errors due to detector gain shifts, changes in the background, and other time-dependent effects. For the simulations above, the

sample was only 0.042 cm in diameter. In a typical experiment, the collimator would be this diameter, while the sample would be slightly larger to allow for positioning errors during sample cycling. I do not know how accurately the sample can be repositioned several hundred times over the course of a typical experiment. Note that transmission measurements for ^{249}Cf and ^{249}Bk were made at ORELA in 1975 using a collimator only 3 times larger (collimator diameter 1.29 mm and sample diameter 1.638±0.010 mm) than in the above simulations. Assuming it is not possible to do any better than this almost 40 years later, the sample would have to be about 3 times larger than estimated above. On the other hand, given the smallness of the sample and the relatively compact neutron source size, it may be possible to design a collimation system so that sample-in and sample-out are run simultaneously on the same flight path. This would alleviate repositioning errors (and hence allow smaller samples to be used) and cut the running time of the experiment approxmately in half.

C. Backgrounds

The above simulations do not include any backgrounds. At ORELA, the largest background was due to ambient (constant in time) events. In principle, because the duty factor at MLNSC is much lower than at ORELA (20 vs. 525 Hz), the ambient background should be much lower at MLNSC than at ORELA. However, the ambient background may be predominantly beam related. It will depend on factors such as the effectiveness of the beam dump and how well the detector is shielded from other flight paths.

V. OUTLOOK

Test experiments to measure actual counting rates and study backgrounds would be relatively easy to implement on, for example, flight path 5 at the MLNSC. Table I contains a list of nuclides of interest to s-process nucleosynthesis studies and radiochemical diagnostics, compiled from similar lists created by Franz Käppeler and Jerry Wilhelmy several years ago. The astrophysics priority in this table is on a scale of 1 (highest) to 4 (lowest). Column 4 contains a check mark if the nuclide has been identified as having a capture cross section of interest to radiochemical diagnostics.

At the MLNSC, the proposed technique works best for nuclides having small D_0 values, so that sufficient resonances can be observed before the relatively poor time-of-flight resolution begins to make it impossible to discern individual resonances. Even with this limitation, there still are many candidate nuclides. The D_0 values in Table I were calculated using the default level-density model in TALYS [6]. As a rough rule of thumb, transmission measurements at MLNSC likely will yield useful constraints on the capture cross section for case where D_0 is less than about 20 eV. Over half the nuclides in Table I satisfy this condition and are highlighted in bold. Of the 43 (19) nuclides of interest to nuclear astrophysics (radiochemical diagnostics) in this table, 24 (11) should be measurable at MLNSC. If pulse stacking becomes a reality, the improved time-of-flight resolution will put even more samples of interest within reach.

The largest remaining uncertainty (in the NSM prediction of the capture cross section) in most cases is likely to be the p-wave neutron strength function S_1. However this parameter can likely be constrained to sufficient accuracy by systematics, or by measuring the average transmission in the unresolved region.

As many of the nuclides of interest identified ~ 20 years ago remain unmeasured, it should be possible to build a strong case for this new capability.

[1] C. E. Porter and R. G. Thomas, Phys. Rev. **104**, 483 (1956).
[2] S. Hilaire, C. Lagrange, and A. J. Koning, Annals of Physics **306**, 209 (2003).
[3] G. J. Kirouac and H. M. Eiland, Phys. Rev. C **11**, 895 (1975).
[4] T. Fuketa and J. A. Harvey, Nucl. Instrum. Methods **33**, 107 (1965).
[5] S. F. Mughabghab, *Atlas of Neutron Resonances: Resonance Parameters and Thermal Cross Sections Z=1-100* (Elsevier, Amsterdam, The Netherlands, 2006).
[6] A. J. Koning, S. Hilaire, and M. C. Duijvestijn, in *Proceedings of the International Conference on Nuclear Data for Science and Technology - ND2007*, edited by O. Bersillon *et al.* (EDP Sciences, Les Ulis, France, 2008), p. 211.
[7] U. Abbandanno *et al.*, Phys. Rev. Lett. **93**, 161103 (2004).
[8] K. Wisshak *et al.*, Phys. Rev. C **73**, 015802 (2006).
[9] R. Reifarth *et al.*, in *10th Sumposium on Nuclei in the Cosmos* (Pos-Proceedings of Science, ADDRESS, 2008).
[10] P. E. Koehler, Nucl. Instr. and Meth. **A292**, 541 (1990).
[11] http://www.detectors.saint gobain.com/ (unpublished).
[12] N. M. Larson, Technical Report No. ORNL/TM-9179/R8, Oak Ridge National Laboratory (unpublished).

TABLE I: Radionuclides of interest to nuclear astrophysics and radiochemical diagnostics. Transmission measurements at the MLNSC should be possible for those nuclides highlighted in bold.

Nuclide	$t_{\frac{1}{2}}$	Astro. priority	Radchem. Interest	D_0 (eV)
^{60}C	5.27 y	4		600
^{63}Ni	100 y	3		2200
^{79}Se	$<6.5\times10^4$ y	1	✓	57
^{85}Kr	10.7 y	1	✓	190
^{86}Rb	18.8 d	1		68
^{88}Y	106.6 d	4		22
^{89}Sr	50.5 d	2/3		920
^{90}Sr	28.8 y	2/3		7700
^{95}Zr	64.0 d	1	✓	198
^{94}Nb	2×10^4 y	2		30
^{95}Nb	35.0 d	2/3		34
^{106}Ru	367 d	2/3		580
^{107}Pd	10^6 y	-	✓	11
^{110m}Ag	252 d	2		4.0
^{119m}Sn	250 d	-	✓	90
^{134}Cs	2.062 y	1/2	✓	11
^{135}Cs	3×10^6 y	2	✓	71.3
^{137}Cs	30.17 y	2/3		1543
^{141}Ce	32 d	-	✓	65
^{147}Nd	11.0 d	1/2		3.5
^{147}Pm	2.62 y	1	✓	5.2
^{152}Eu	13.3 y	1	✓	0.5
^{154}Eu	8.5 y	1		0.9
^{155}Eu	4.9 y	1	✓	4.3
^{153}Gd	241.6 d	1	✓	0.6
^{160}Tb	72.1 d	1/2		0.7
^{161}Tb	6.9 d	2/3		3.1
^{163}Ho	≈33 y	1	✓	0.7
^{166}Ho	1200 y	2/3		8.6
^{169}Er	9.40 d	1/2		18
^{170}Tm	128.6 d	1	✓	3.9
^{171}Tm	1.92 y	1		6.3
^{175}Yb	4.19 d	2		8.3
^{179}Ta	1.7 y	1		0.6
^{181}Hf	4.4 d	2/3		25
^{182}Hf	9×10^6 y	2/3		130
^{185}W	75.1 d	1	✓	6.3
^{186}Re	90.6 h	1	✓	1.6
^{191}Os	15.4 d	1/2		3.4
^{192}Ir	74.2 d	1/2	✓	0.5
^{193}Pt	50 y	1/2	✓	5.8
^{198}Au	2.69 d	2		12.1
^{203}Hg	46.8 d	1		323
^{205}Pb	10^7 y	-	✓	370
^{204}Tl	3.77 y	1		216
^{210m}Bi	3.0×10^6 y	2/3		2048
^{210}Bi	5.01 d	2/3		2048